

# Feature Matching using Supersymmetric Geometric Constraints

## Abstract

Feature matching is a challenging problem lying at the heart of numerous computer graphics and computer vision applications. We present here the *SuperMatching* feature matching algorithm for finding correspondences between two sets of features. *SuperMatching* finds matches of feature points by considering triangle or higher-order polygons formed by such points, going beyond the pointwise and pairwise approaches typically used. It is formulated as a supersymmetric-tensor-based matching scheme, casting feature matching as a higher-order graph matching problem. The supersymmetric tensor represents an affinity metric which takes into account geometric constraints between features. *SuperMatching* exploits a compact form of this affinity tensor, whilst also taking advantage of supersymmetry to devise an efficient sampling strategy to create the affinity tensor. Matching is performed by computing a rank-one approximation of the tensor directly using a higher-order power solution method. Experiments on both synthetic and real captured data show that our algorithm provides accurate feature matching even in complex cases.

**Keywords:** Feature matching; Geometric constraints; Supersymmetric tensor

## 1 Introduction

Building correspondences between two sets of features of 2D/3D shapes is a fundamental problem in many geometric processing, computer graphics and computer vision tasks. It arises in applications such as feature extraction [Johnson and Hebert 1999; Lowe 2004; Sun et al. 2009; Bokeloh et al. 2008; Toler-Franklin et al. 2010; Leutenegger et al. 2011], shape matching [Berg et al. 2005; Brown and Rusinkiewicz 2007; Torresani et al. 2008; Tevs et al. 2009; Ovsjanikov et al. 2010; Tevs et al. 2011; Sahillioglu and Yemez 2011; Windheuser et al. 2011], registration of 3D shapes [Gelfand et al. 2005; Aiger et al. 2008; Li et al. 2008; Zeng et al. 2010; van Kaick et al. 2011; Chang and Zwicker 2011], automatic shape understanding [Lipman and Funkhouser 2009; Sun et al. 2010; Kim et al. 2011], shape retrieval from database [Bronstein et al. 2011], and reconstruction [Brown and Rusinkiewicz 2007; Pekelny and Gotsman 2008; Wand et al. 2009; Chang and Zwicker 2011].

In principle and practise, the correspondence building process mainly proceed in three steps [Lowe 2004; Leutenegger et al. 2011]: salient feature detection, high-quality descriptor, and accurately matching. The former two problems have been widely attracted considerable attention as their importance is easy perceivable. However, even with the ideal feature detector and descriptor that capturing the most important and distinctive information content enclosed in the detected salient regions, the correspondences still could not ideally built in the state-of-the-art algorithms [van Kaick et al. 2011]. The reason is that the real input data is so imperfect and complex especially with symmetric and repetitive regions. The researchers are beginning to be aware of that the limitation could be effectively alleviated by feature matching. Some original idea (e.g. RANSAC-like algorithms [Tevs et al. 2009; Tevs et al. 2011]) has been extended, or indirectly sorting to shape embedding

strategies, such as Generalized Multidimensional Scaling [Bronstein et al. 2011], Heat Kernel Map [Ovsjanikov et al. 2010], Möbius Transformation [Lipman and Funkhouser 2009; Kim et al. 2011]. But, these previous algorithms still did not treat feature matching as one independent problem, although they agreed with that matching is not tightly coupled with feature detection and description.

In the paper, we mainly focus on feature matching problem, which is complementary to existing feature detection and description algorithms. As we know, a matching itself may comprise one or more items of a given kind. We may match single point to single point (point-single), point pairs separated by a fixed distance to other point pairs (segment-double), triples of points forming a triangle to other triples of points (triangle-triple), quadruples of points forming a quadrangle to other quadruples of points (quadrangle-quadruple), and so on. As pointed by [Conte et al. 2004], when single features are matched, we must solve a linear assignment problem, if multiple features are matched at once, a quadratic or higher-order assignment problem results.

Linear assignment matches single features in one set with single features in the other set, and could be mainly treated as single points linkage. Matching two feature sets by considering similarities of *single* features from each set can easily fail in the presence of ambiguities such as repeated elements, or similar local appearance.

Quadratic and higher-order assignment matches groups of features in one set simultaneously with groups from the other set, and requires a greater consistency between the information being matched, making it more reliable. As well as the features themselves, other constraints such as consistency of the distances between the features being matched are also enforced, greatly improving the matching accuracy.

As a particular example of *quadratic* assignment, Leordeanu and Hebert [Leordeanu and Hebert 2005] consider pairs of feature descriptors, and distances between pairs of features from each set to reduce the number of incorrect correspondences. Such pairwise distance constraints are particularly helpful in cases when the features themselves have low discriminative ability. The idea has been widely adopted in the 3D shape matching algorithms [Tevs et al. 2009; Ovsjanikov et al. 2010; Tevs et al. 2011; Kim et al. 2011; Sahillioglu and Yemez 2011; Windheuser et al. 2011].

Higher-order assignment further generalizes the assignment problem to include yet more complex constraints between features. For example, third-order potential functions, proposed in [Duchenne et al. 2009; Zeng et al. 2010; Chertok and Keller 2010], quantify the affinity between two point triples by measuring the similarity of the angles formed by such two feature tuples (triangles). However, this angular similarity value only calculates the total differences in corresponding angles, and does not change with the order of the input assignments. By changing the affinity tensor to a *supersymmetric* tensor [Kofidis and Regalia 2002], the unaccurate limitation could be further solved by our algorithm.

Thus, by formulating the higher-order problem using a supersymmetric affinity tensor, we propose a general higher-order supersymmetric matching algorithm, named *SuperMatching*. *SuperMatching*, addressed in Section 4, which accurately matching a moderate number of features using triples or higher polygons of features. The contributions of this paper include:

- We show how to define a compact higher-order supersymmetric affinity tensor to express geometric consistency constraints between tuples of features.
- Based on the supersymmetry of the affinity tensor, we propose a higher-order power iteration method, which efficiently solves the matching problem.
- The affinity tensor is physically created by using a new efficient sampling strategy for feature tuples, which avoids sampling repetitive items, reduces the number of feature tuples to be sampled while improving the matching accuracy.

Our experiments in Section 5 on both synthetic and real captured data sets show that SuperMatching result is accurate and robust, and has competitive computational cost compared to previous algorithms. More important, the matching is performed by incorporating variant 2D and 3D feature descriptors, which demonstrate that SuperMatching is independent on descriptors and could be generally applied in computer graphics and computer vision fields.

## 2 Related work

According to the applied constraints, previous approaches to feature matching can be classified into those which match single points to single points, those which match pairs of points to pairs of points, and so on.

Matching single points to single points is a linear assignment problem which only considers an affinity measure between two graph nodes, one from each set being matched; this measure is typically the feature distance between the two feature points. Affinity measures used in computer vision and computer graphics tasks rely heavily on descriptors computed using local information around each feature point, e.g. SIFT [Lowe 2004], spin images [Johnson and Hebert 1999], slippage features [Bokeloh et al. 2008], heat diffusion signatures [Sun et al. 2009], and BRISK [Leutenegger et al. 2011]. It is apparent that point-to-point matching is weak in that wrong correspondences maybe readily be established.

Matching pairs of points in one set to pairs of points in the other set leads to a quadratic assignment problem. The usual approach is now to take into account both similarity of the point features and the Euclidean/Geodesic distance between the points in a pair, assuming the objects are related by a rigid transformation [Leordeanu and Hebert 2005; Cour et al. 2006], or at least an isometry [Li et al. 2008; Tevs et al. 2009; Ovsjanikov et al. 2010; Tevs et al. 2011; Sahillioglu and Yemez 2011; Windheuser et al. 2011]. The quadratic assignment problem seeks to find a mapping which represents the optimal assignment. Unfortunately, this problem is NP-hard, unreasonable matching results could not be avoided.

Several higher-order approaches have also been proposed. Such higher-order methods can significantly improve matching accuracy, but higher-order assignment problem is more challenging, and various approximate methods have again been developed. Zass and Sashua [Zass and Sashua 2008] consider a probabilistic model of soft hypergraph matching. They reduce the higher-order problem to a first-order one by marginalizing the higher-order tensor to a one dimensional probability vector. Duchenne et al. [Duchenne et al. 2009] introduced a third-order tensor in place of an affinity matrix to represent affinities of feature triples, and higher-order power iteration was used to achieve the final matching. Chertok et al. [Chertok and Keller 2010] treat the tensor as a joint probability of assignments, marginalize the affinity tensor to a matrix, and find optimal soft assignments by eigendecomposition of the matrix. Wang et al. [Wang et al. 2010] also build a third-order affinity tensor, and obtain a final matching by rank-one approximation of the tensor.

Higher-order assignment problems typically require large amounts of memory and computational resources. By reducing the number of elements needed to represent the affinity measures, the above approaches can match moderate numbers (many hundreds or more) of features. However, these 2D approaches still did not use the advantage of supersymmetric tensor, leading to a reduction in matching accuracy. For the harder 3D applications, there exists so many unpredictable issues.

A related idea using higher constraints in 3D registration, 4-points congruent sets method (4PCS), was proposed by Aiger et al. [Aiger et al. 2008]. It is a fast alignment scheme for 3D point sets that uses widely separated points. However, the coplanar 4 points and rigid-transformation constraints are some strong, and limit its application. We solve both rigid and isometric shape matching problem by one more mathematical and formulated tensor-based algorithm.

## 3 Overview

Assume we are given two sets of feature points  $P_1$  and  $P_2$ , with  $N_1$  and  $N_2$  points respectively. The matching between these two feature sets can be represented by an *assignment matrix*  $X$  of size  $N_1 N_2$  whose elements are 0 or 1.  $X(i, j) = 1$  when  $i \in P_1$  matches  $j \in P_2$  and  $X(i, j) = 0$  otherwise.  $X$  can be row-wise vectorized to give an assignment vector  $\mathbf{x} \in \{0, 1\}^{N_1 N_2}$ .

Solving the higher-order matching problem is equivalent to find the optimal assignment vector  $\mathbf{x}^* = \langle x_{i_1}, \dots, x_{i_N} \rangle \in \{0, 1\}^{N_1 N_2}$ , satisfying

$$\mathbf{x}^* = \arg \max_{\mathbf{x}} \sum_{i_1, \dots, i_N} \mathcal{T}_N(i_1, \dots, i_N) x_{i_1} \dots x_{i_N}. \quad (1)$$

Here,  $i_n$  stands for an assignment  $(i'_n, j'_n)$ , ( $i'_n \in P_1, j'_n \in P_2$ ), and the product  $x_{i_1} \dots x_{i_N}$  is 1 only if all assignments  $\{i_n\}_{n=1}^N$  are equal to 1, which means the tuple of features  $(i'_1, \dots, i'_N)$  from  $P_1$  is matched correspondingly to the tuple of features  $(j'_1, \dots, j'_N)$  from  $P_2$ .  $\mathcal{T}_N(i_1, \dots, i_N)$  defines the affinity of the set of assignments  $\{i_n\}_{n=1}^N$ ; it also can be seen as the affinity measure between the ordered feature tuples  $(i'_1, \dots, i'_N)$  and  $(j'_1, \dots, j'_N)$ .

In the paper, we consider the one-to-many correspondence problem. We assume that a point in  $P_1$  is matched to exactly one point in  $P_2$ , but that the reverse is not necessarily true. If *do* we want to treat both datasets in the same way, we can first match  $P_1$  to  $P_2$ , then match  $P_2$  to  $P_1$ , and then combine the matching results by taking their union or intersection. Uniqueness of matches for  $P_1$  means that the assignment matrix  $X$  satisfies  $\sum_i X(i, j) = 1$ .

From Equ.(1) we can see that there are four issues to be considered when using higher-order matching algorithms. How should we:

- organize and express the affinity measures  $\mathcal{T}_N$ ? (see Section 4.1)
- approximately solve the optimal higher-order assignment problem efficiently? (see Section 4.2)
- define the affinity measure between two feature tuples, or equivalently, the higher-order potential function  $\phi_N$ ? (see Section 4.3)
- determine an appropriate sampling strategy that physically build the affinity tensor and influence good matching accuracy? (see Section 4.4)

## 4 SuperMatching

We first discuss the former two issues mentioned above, which are independent of application; later we turn to definition of affinity measure, which is application dependent, and sampling strategy.

### 4.1 Supersymmetric affinity tensor

A tensor generalises vectors and matrices to higher dimensions: a vector is a tensor of order one, and a matrix is a tensor of order two. A higher-order tensor can be expressed as a multi-dimensional array [Kolda and Bader 2009]. Here we consider a higher-order supersymmetric affinity tensor, which represents a real-valued higher-order affinity between feature tuples.

**Definition 1 (Supersymmetric Tensor)** A tensor is called supersymmetric if its entries are invariant under any permutation of its indices [Kofidis and Regalia 2002].

For example, a third-order supersymmetric tensor  $\mathcal{T}_3$ , satisfies the relationships:  $\mathcal{T}_3(i_1, i_2, i_3) = \mathcal{T}_3(i_1, i_3, i_2) = \mathcal{T}_3(i_2, i_1, i_3) = \mathcal{T}_3(i_2, i_3, i_1) = \mathcal{T}_3(i_3, i_1, i_2) = \mathcal{T}_3(i_3, i_2, i_1)$ .

**Definition 2 (Supersymmetric Affinity Tensor)** Given two feature sets  $P_1$  and  $P_2$ , with  $N_1$  and  $N_2$  features respectively, the supersymmetric affinity tensor is an  $N^{th}$  order  $I_1 \cdots \times I_N$ , nonnegative tensor  $\mathcal{T}_N$ , where  $I_1 = I_2 = \cdots = I_N = \{1, \dots, N_1 N_2\}$ , for which there exists a set of indices  $\theta_N$ , and an  $N^{th}$  order potential function  $\phi_N$ , such that

$$\mathcal{T}_N(i_1, \dots, i_N) = \begin{cases} \phi_N(\Omega(i_1, \dots, i_N)) & , \forall (i_1, \dots, i_N) \in \theta_N \\ 0 & , \forall (i_1, \dots, i_N) \notin \theta_N \end{cases} \quad (2)$$

where  $\Omega$  stands for an arbitrary permutation of the vector, and  $\theta_N$  satisfies  $\forall (i_1, i_2, \dots, i_N) \in \theta_N, \forall i_p \in \{i_1, \dots, i_N\}$  and  $\forall i_q \in \{i_1, \dots, i_N\} - \{i_p\}$  meets the requirement that  $i_p \neq i_q$ .

A tensor element with  $(i_1, i_2, \dots, i_N) \in \theta_N$  is called a potential element, while other elements are called non-potential element.

Using Definition 2, we now can greatly reduce the amount of storage needed, representing every potential element  $\mathcal{T}_N(i_1, i_2, \dots, i_N)$  by the canonical entry  $\mathcal{T}_N(\text{sort}(i_1, i_2, \dots, i_N))$ ,  $\forall (i_1, i_2, \dots, i_N) \in \theta_N$ . Each stored value thus provides the value for  $N!$  entries. As non-potential elements all have value zero, there is no need to store them. This greatly reduces the sampling needed for feature tuples when creating the affinity tensor, as discussed in Section 4.4. At the same time, it can be used to make the power iteration process more efficient: see Section 4.2.

### 4.2 Higher-order Power Iteration Solving

Using Definition 2, Equ.(1) can be expressed as:

$$\begin{aligned} \mathbf{x}^* &= \arg \max_{\mathbf{x}} \sum_{i_1, i_2, \dots, i_N} \mathcal{T}_N(i_1, \dots, i_N) x_{i_1} \cdots x_{i_N} \\ &= \max \langle \mathcal{T}_N, \mathbf{x}^{\star N} \rangle \end{aligned} \quad (3)$$

where  $\star$  is called the Tucker product [Kofidis and Regalia 2002], and  $\mathbf{x} \in \{0, 1\}^{N_1 N_2}$ . Solving Equ.(3) is an NP-complete problem, so it is common to relax the constraints: the binary assignment vector  $\mathbf{x} \in \{0, 1\}^{N_1 N_2}$  is replaced by an assignment vector  $\mathbf{u}$  with elements taking real values in  $[0, 1]$ . This changes the optimization problem to one of computing the rank-one approximation of the affinity tensor  $\mathcal{T}_N$  [Kofidis and Regalia 2002], i.e.

**Algorithm 1** Higher-order power iteration method for a supersymmetric affinity tensor (with  $C_1$  norm)

**Input:**  $N$ th-order supersymmetric affinity tensor  $\mathcal{T}_N$   
**Output:** unit-norm vector  $\mathbf{u}$

```

1: Initialize  $\mathbf{u}_0, k = 1$ 
2: repeat
3:   for all  $(i_1, i_2, \dots, i_N) \in \theta_N$  do
4:     for all  $m \in (i_1, \dots, i_N)$  do
5:        $v_m^{(k)} = (N-1)! \phi_N(i_1, \dots, i_N) 2v_m^{(k-1)} v_{i_1}^{2(k-1)} \dots$ 
          $v_{m-1}^{2(k-1)} v_{m+1}^{2(k-1)} \dots v_{i_N}^{2(k-1)}$ 
6:     end
7:     for  $i = 1 : N_1$  do
8:        $v^{(k)}(((i-1) \cdot N_2 + 1) : i \cdot N_2) =$ 
          $\hat{v}^{(k)}(((i-1) \cdot N_2 + 1) : i \cdot N_2) / \|\hat{v}^{(k)}(((i-1) \cdot N_2 + 1) :$ 
          $i \cdot N_2)\|_1$ 
9:     end
10:    end
11:     $k = k + 1;$ 
12: until convergence;
Note:  $v^{(k)}(((i-1) \cdot N_2 + 1) : i \cdot N_2)$  denotes the slice of  $v^{(k)}$  with indices from  $(i-1) \cdot N_2 + 1$  to  $i \cdot N_2$ .
```

finding a scalar  $\lambda$  and a unit norm vector  $\mathbf{u} \in \mathbb{R}^{N_1 N_2}$ , such that the tensor  $\hat{\mathcal{T}}_N = \lambda \mathbf{u} \star \mathbf{u} \star \cdots \star \mathbf{u} = \mathbf{u}^{\star N}$  minimizes the function  $f(\hat{\mathcal{T}}_N) = \|\mathcal{T}_N - \hat{\mathcal{T}}_N\|$ . The final matching result is found by replacing each element of  $\mathbf{u}$  by 0 or 1 according to whichever it is closer to.

The higher-order power method is commonly used to find the rank-one tensor approximation; a version for supersymmetric tensors (S-HOPM) is given in [Kofidis and Regalia 2002]. The S-HOPM algorithm converges under the assumption of convexity for the functional induced by the tensor [Kofidis and Regalia 2002], which is so robust that could be satisfied in practical application. S-HOPM is performed in two iterative steps: high-order power iteration of  $\mathbf{u}$ , normalization of  $\mathbf{u}$  under the Frobenius norm. In the recent, one more effective improvement [Duchenne et al. 2009] was proposed by using  $C_1$  norm to replace the traditional  $C_2$  norm.

We directly take the  $C_1$  norm [Duchenne et al. 2009] and further revise S-HOPM as following. For the first step (high-order power

iteration of  $\mathbf{u}$ ),  $\hat{\mathbf{u}}^{(k)} = \mathcal{I} \overset{\mathcal{T}_N}{\star} (\mathbf{u}^{(k-1)})^{\overset{\mathcal{T}_N}{\star} (N-1)}$ ,  $\overset{\mathcal{T}_N}{\star}$  is a so-called  $\mathcal{T}_N$ -product,  $\mathcal{I}$  is the unit tensor [Kofidis and Regalia 2002]. Then, for  $\hat{\mathbf{u}}^{(k)}$  with  $N$ th-order supersymmetric affinity tensor, it can be formulated as:

$$\begin{aligned} \hat{\mathbf{u}}^{(k)} &= \mathcal{I} \overset{\mathcal{T}_N}{\star} (\mathbf{u}^{(k-1)})^{\overset{\mathcal{T}_N}{\star} (N-1)} \Leftrightarrow \\ \forall m \in (i_1, \dots, i_N), v_m^{(k)} &= \\ \sum_{i_1, \dots, i_N} \mathcal{T}_N(i_1, \dots, i_N) 2v_m^{(k-1)} v_{i_1}^{2(k-1)} \dots v_{m-1}^{2(k-1)} v_{m+1}^{2(k-1)} \dots v_{i_N}^{2(k-1)} &= \\ (N-1)! \phi_N(i_1, \dots, i_N) 2v_m^{(k-1)} v_{i_1}^{2(k-1)} \dots v_{m-1}^{2(k-1)} v_{m+1}^{2(k-1)} \dots v_{i_N}^{2(k-1)} &= \end{aligned} \quad (4)$$

where  $\mathbf{u}^{(k)} = \mathbf{v}^{(k)}$ ,  $\phi_N$  is corresponding potential function. The deduction relies on two principles. First, we take advantage of the supersymmetry. Secondly, many of the elements of the affinity tensor are zero non-potential elements: it is much more efficient to perform the power iteration by just considering the non-zero potential elements. So, our supersymmetric higher-order power iteration solving is addressed as Algorithm 1.

This version excludes each non-potential element from the iteration process, so is more efficient, and the complexity of the whole iteration process only depends on the number  $|\theta_N|$  of affinities. Step 5

in Algorithm 1 includes all permutations of each potential element  $\mathcal{T}_n(i_1, i_2, \dots, i_n)$ , which are expressed by a single potential function  $\phi_n(i_1, i_2, \dots, i_n)$ . Consequently, This method reduces memory costs while keeping accuracy. Please noted that, although the affinity tensor [Duchenne et al. 2009] was claimed as supersymmetric. [Duchenne et al. 2009] did not make full use of supersymmetry when creating the supersymmetric affinity tensor, nor did they take advantage of supersymmetry when accelerating the power iteration process. Fortunately, the limitation due to unbalanced and redundant tensor elements in [Duchenne et al. 2009] could be overcome by Algorithm 1. The later experiment proves the expectation.

Many initialization schemes have been proposed for S-HOPM method [Kofidis and Regalia 2002]. We simply use positive random values to initialize  $\mathbf{u}_0$ , which ensures the algorithm's convergency.

### 4.3 Higher-order Potentials

Different higher-order potentials are appropriate for different applications. Here we give two general higher-order potentials. One is used for the 2D cases, while the other is defined for 3D matching. The potentials are based on a Gaussian kernel which guarantees the tensor elements are non-negative and invariant to any permutation of the input assignments.

In 2D cases, we first restate a well-known 2D third-order geometric-similarity invariant potential  $\phi_3$  [Duchenne et al. 2009; Chertok and Keller 2010] linking two feature tuples, each having three features. Similarity of triangles formed by three points corresponds to invariance under scaling, rotation and translation—interior angles do not change. Thus  $\phi_3$  can be defined in terms of differences of corresponding interior angles:

$$\begin{aligned} \phi_3(i, j, k) &= \phi_3(\{i_1, i_2\}, \{j_1, j_2\}, \{k_1, k_2\}) \\ &= \exp(-1/\varepsilon^2 \sum_{(l, l')} \|\alpha_l - \alpha_{l'}\|^2) \end{aligned} \quad (5)$$

where  $\varepsilon > 0$  is the kernel bandwidth,  $\{\alpha_l\}_{l=1}^3$  and  $\{\alpha_{l'}\}_{l'=1}^3$  are the angles formed by feature triples  $(i_1, j_1, k_1)$  and  $(i_2, j_2, k_2)$ : see figure 1. Each element corresponds to one interior angle. We extend it to all general cases by using the internal angles formed by the triangle and higher polygons. It is easy to understand that the potential preserves invariance under rigid transformations in 2D field.

For 3D matching problem, we replace the internal angle by edge length, i.e., the geodesic distance between two neighboring points. The geodesic distance [Peyré et al. ] between two points is computed by the shortest Dijkstra algorithm. Therefore, the feature matching is performed using the geometric constraints with invariance, which going beyond traditional the single (point) and pairwise features.

We will use these two high-order potentials to evaluate our algorithm. Figure 1 illustrates the schematic diagram of third-order potential in 2D and 3D cases.

### 4.4 Sampling strategy

Algorithm 1 depends on all potential elements. We next discuss the issue of how to sample the feature tuples to build potential items, which determines the size  $|\theta_N|$  and influences matching accuracy.

Given two feature sets  $P_1$  and  $P_2$  with  $N_1$  and  $N_2$  features respectively, a potential element may be obtained by using two feature tuples sampled from each feature set separately. For  $N$ -th-order matching, a naive way to construct the potential elements is as follows: first find all feature tuples for  $P_1$  and  $P_2$ , as  $F_1$  and

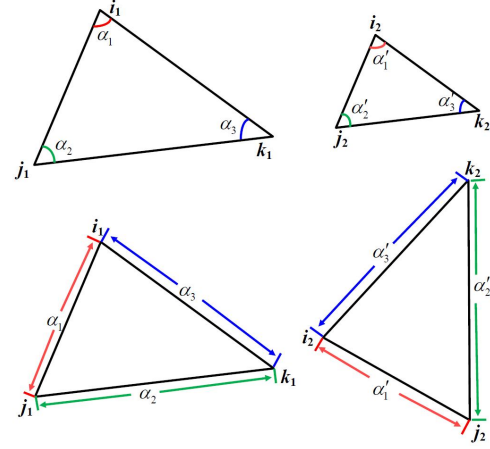


**Figure 1:** Third-order potential schematic diagram. The geometric constraints: internal angle invariance in 2D (up), and edge length invariance in 3D case (bottom).

$F_2$ ; then  $\forall (f_{i_1}^1, f_{i_2}^1, \dots, f_{i_N}^1) \in F_1$ , calculating the potentials for  $(f_{i_1}^1, f_{i_2}^1, \dots, f_{i_N}^1)$  with all feature tuples in  $F_2$ . This naive method is very expensive, which is why sampling is used. Different sampling strategies can be chosen for different applications, we employ random sampling for general feature matching problems.

Our sampling works as following: randomly sampling  $t_1$  feature tuples for  $P_1$ , and full sampling for  $P_2$  (to find all  $N_2^{t_1}$  feature tuples). For  $P_1$ , in order to cover all features in  $P_1$  in  $F_1$ , we repeatedly take one feature as a required element, and then randomly choose  $t_1$  feature tuples containing these required element. We repeat this process until all features in  $P_1$  have been chosen once as a required element. Then,  $\forall (f_{i_1}^1, f_{i_2}^1, \dots, f_{i_N}^1) \in F_1$ , we find the  $k$  most similar features in  $F_2$  to build  $k$  potential elements as  $\phi_i^k$ . Combining all the potential elements obtained, we form the desired potential element set  $\theta_N = \{\phi_i^k\}_{i=1}^{N_1 t_1}$ , with the size  $|\theta_N| = N_1 t_1 k$ . The parameters  $t_1$  and  $k$  must be chosen according to the size of the feature sets. For  $P_1$ , the sampling cost is  $O(N_1 t_1 \log N_1)$ . In practice, for two feature sets each with hundreds points, we take  $t_1 \approx 100$  and  $k \approx 300$  for third-order and higher-order (e.g. fourth-order) matching. The experiments demonstrate that this sampling approach works well.

The most important part of the sampling is to use the supersymmetry of the affinity tensor. An  $N^{th}$ -order supersymmetric affinity tensor must satisfy:

$$\begin{aligned} \forall (i_1, i_2, \dots, i_N), (j_1, j_2, \dots, j_N) \in \theta_N, \\ (i_1, i_2, \dots, i_N) \neq \Omega(j_1, j_2, \dots, j_N) \end{aligned} \quad (6)$$

where  $\Omega$  is an arbitrary permutation. Thus, we use a sampling constraint that the sets of feature tuples  $F_1$  obtained from the sampling process, should have no repetition, in the sense that

$$\begin{aligned} \forall (f_{i_1}^1, f_{i_2}^1, \dots, f_{i_N}^1), (f_{j_1}^1, f_{j_2}^1, \dots, f_{j_N}^1) \in F_1, \\ (f_{i_1}^1, f_{i_2}^1, \dots, f_{i_N}^1) \neq \Omega(f_{j_1}^1, f_{j_2}^1, \dots, f_{j_N}^1) \end{aligned} \quad (7)$$

and  $\Omega$  is arbitrary permutation. This sampling constraint eliminates overlaps that may appear in the potential elements  $\theta_N$ .

Earlier work [Duchenne et al. 2009; Zass and Shashua 2008] ever adopted random sampling, but failed to impose any constraint on the sampling process, leading to the possibility that feature tuples may include repetition. For example, for third-order matching, it is

possible that a feature tuple  $(f_{i_1}^1, f_{i_2}^1, f_{i_3}^1)$  may be sampled from  $P_1$  and  $(f_{i_1}^2, f_{i_2}^2, f_{i_3}^2)$  from  $P_2$ , and also a feature tuple  $(f_{i_1}^1, f_{i_3}^1, f_{i_2}^1)$  sampled from  $P_1$  and  $(f_{i_1}^2, f_{i_3}^2, f_{i_2}^2)$  from  $P_2$ . That will create two tensor elements  $\phi_3(s_{i_1}, s_{i_2}, s_{i_3})$  with index  $(s_{i_1}, s_{i_2}, s_{i_3})$  and  $\phi_3(s_{i_1}, s_{i_3}, s_{i_2})$  with index  $(s_{i_1}, s_{i_3}, s_{i_2})$ , which are the same. However, we just need one tensor element to express the affinity measure on the assignment group  $(s_{i_1}, s_{i_2}, s_{i_3})$ . This repetitive problem not only makes the potential elements redundant but also affects the accuracy of the power iteration, because the numbers of each tensor element may not be equal and some elements may be used more than once during the iteration progress. Therefore, our sampling method reduces the sampling cost, while also improving the accuracy of the power iteration.

## 5 Experiments

We have used synthetically generated data as well as real captured data to evaluate the SuperMatching algorithm. To demonstrate the independence and generalization of the SuperMatching, different descriptors have been applied. For 2D deformable surface, SIFT [Lowe 2004] are used. While for the 3D shapes without color information, slippage features [Bokeloh et al. 2008] are employed. For 3D colorful shapes, both SIFT and slippage features are employed. To build the matching between two shapes, we used third-order matching for the experiments. For greater than third higher-order, it is easy to replace the potential by relevant polygonal definitions.

### 5.1 2D deformable surfaces

Firstly, we used a 2D deformable surface data<sup>1</sup> with a cloth and a cushion. The surfaces of the cloth underwent relatively smooth deformations, while the surfaces of the cushion included sharp folds. The data has provided ground truth, which are very useful to verify the accuracy quantitatively. From each image set we randomly chose six frames before and after a large deformation. We randomly chose 100 corresponding points on each surface to be the features, using the provided ground truth. In each image set we chose the features on the frame most unlike the others as  $P_1$  and matched them with the features in the other five frames.

We used the data as a basis for comparison with the spectral algorithm [Cour et al. 2006] (a quadric assignment algorithm), a third-order tensor algorithm [Duchenne et al. 2009], and the hyper graph matching algorithm [Zass and Shashua 2008], using the authors' code in each case. All methods were executed in Matlab on a 2.3GHz Core2Duo with 2GB memory. To enable direct and fair comparison, [Duchenne et al. 2009], [Zass and Shashua 2008] and SuperMatching used the same potential and all maintained an equivalent tensor size.

In the tests, SuperMatching used 20000 feature tuples, while the method of [Duchenne et al. 2009] used 1010000 features and the method of [Zass and Shashua 2008] used 40000. The difference is mainly resulting from the effects of sampling strategy, and it could prove that our sampling is effective to reduce the sampling cost. The average running time to match two feature sets each with 100 features was around 8s for SuperMatching, 13s for [Duchenne et al. 2009], 6.5s for [Zass and Shashua 2008], and 5s for [Cour et al. 2006]. So, as we use same tensor size but fewer feature tuples, SuperMatching is performed with less computation than third-order tensor algorithm [Duchenne et al. 2009].

The matching accuracy is given as the number of correctly matched points (according to the provided ground truth) divided by the total

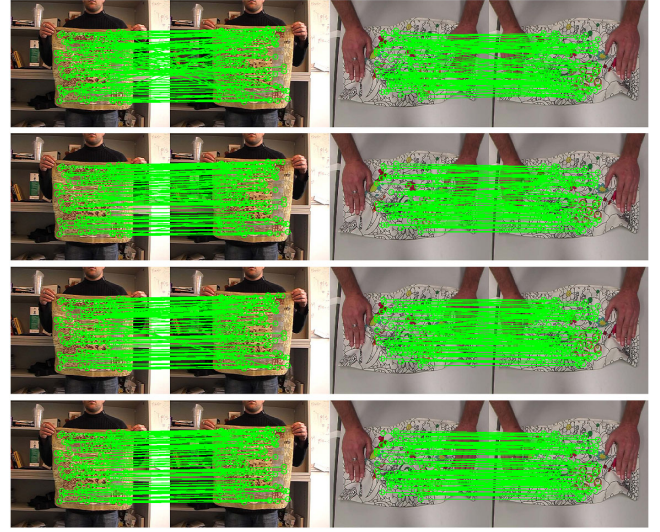


**Figure 2:** Matching results. Left: cloth set, selected from frame 85 to 110, right: cushion set, selected from frames 144 to 213. Top to bottom, spectral method [Cour et al. 2006], hyper graph matching method [Zass and Shashua 2008], a Third-order tensor [Duchenne et al. 2009], and our SuperMatching algorithm.

**Table 1:** Error rate of deformable surface matching.

Dataset	cloth				cushion					
Matching frames	F80- F90- F95- F100- F90 F95 F100 F105	F144- F156- F165- F172- F156 F165 F172 F188					Feature Time Tuples (s)			
SuperMatching	17% 15% 16% 19%	34% 40% 31% 44%								
[Zass and Shashua 2008]	27% 21% 30% 28%	56% 61% 46% 57%								
[Duchenne et al. 2009]	33% 23% 27% 35%	61% 69% 53% 58%								
[Cour et al. 2006]	73% 71% 78% 73%	86% 95% 72% 93%								

number of points that could potentially be matched. The results for all algorithms, using the two image sets, are given in Table 1 and are illustrated in Figure2. Table 1 demonstrates that we achieve a higher matching accuracy than previous algorithms. The worst matching result is produced by the spectral quadratic assignment algorithm [Cour et al. 2006], due to the powerless solution from the pairwise geometric constraints. The results also show that higher-order algorithms perform much better due to the more complex geometric constraints. However, the third-order algorithm [Duchenne et al. 2009] and the hyper graph matching algorithm [Zass and Shashua 2008] do not perform well, because the geometric relationships among elements are not established accurately from the symmetric tensor.

### 5.2 3D rigid shape scans

Secondly, we used the SuperMatching to alignment multiple 3D rigid shape scans. For the multiple scans, the Third-order matching is first performed between two consecutive frames. Then rigid transforms can be computed from the three compatible matching feature points. The transform which brings the most data points within a threshold of a point in the model is chosen as the optimal aligning transform [Huttenlocher and Ullman 1990]. As stated by [Gelfand et al. 2005], the voting scheme is guaranteed to find the optimal alignment between the pairwise scans and is independent of the initial pose of the input scans. After the initial pairwise matching, the alignment is refined by the iterative closest point (ICP) algorithm similar to [Gelfand et al. 2005]. Figure 3 demonstrates the former explains. On the up, the sheep head object is captured from

<sup>1</sup>From <http://cvlab.epfl.ch/data/dsr/>



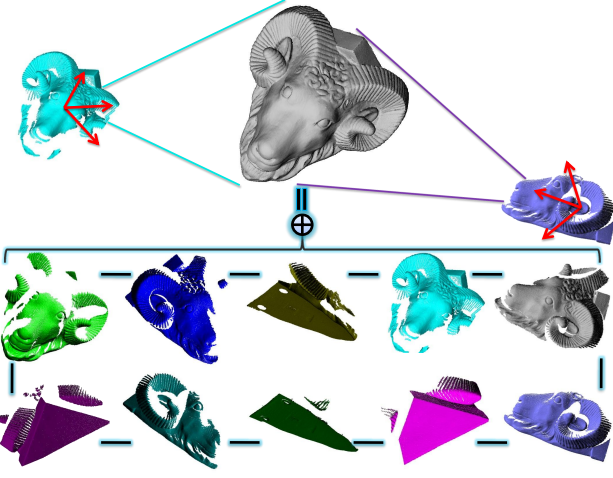


**Figure 3:** The alignment of rigid sheep head scans. The scans are captured from different viewpoints (up), and the final aligned shape is formed from 10 scans (bottom).

different viewpoints, and relevant scans are generated. Relative position and orientation of 10 scans is then be computed to produce a single merged shape. The linkage segments between consecutive scans imply where the SuperMatching algorithm is applied.

### 5.3 3D articulated shape synthetic data

Thirdly, we present another application, articulated registration, to address these challenges by reconstructing an articulated 3D shape from dynamic range scans. Given a sequence of range scans of a moving articulated subject, the method automatically registers all data to produce a complete 3D shape. The advantages of the method is that it does not require any manual segmentation, user specified markers, nor a prior template. Ultimately, the problem of non-rigid registration of deformable shapes is ill-posed and no algorithm is applicable to all scenarios. We believe, however, that our approach pushes the limits of what can be achieved with minimal prior information, and is robust to the partial data with holes.

The articulated registration is performed in two main steps. We first precomputing an initial pairwise registration for each pair of consecutive frames, then the articulated shape reconstruction similar as [Pekelnny and Gotsman 2008]. Although the partial scans have missing data and their poses are different, the SuperMatching could produce accurate matching. Using the correspondences established by the SuperMatching, the robust registration of scans are obtained by computing the piecewise rigid transformations. Then, we propagate the transformations assigned from the slippage feature points subset to all points using nearest neighbor interpolation. The incidental outcomes of pairwise registration include the rigid parts detection by clustering the transformation and segmenting the partial data. The transformation clustering is done by mean shift algorithm [Comaniciu and Meer 2002], which is a robust non-parametric method based on gradient ascent. Therefore, after the initial pairwise registration, the consecutive two partial data has been registered and each data has been segmented according to the transformation. The outcome would be used as the input for the second step articulated shape reconstruction [Pekelnny and Gotsman 2008]. The algorithm identifies and tracks the rigid parts in each frame, while accumulating the geometric information over time. For more details on articulated shape reconstruction with segmentation information, we refer to [Pekelnny and Gotsman 2008].

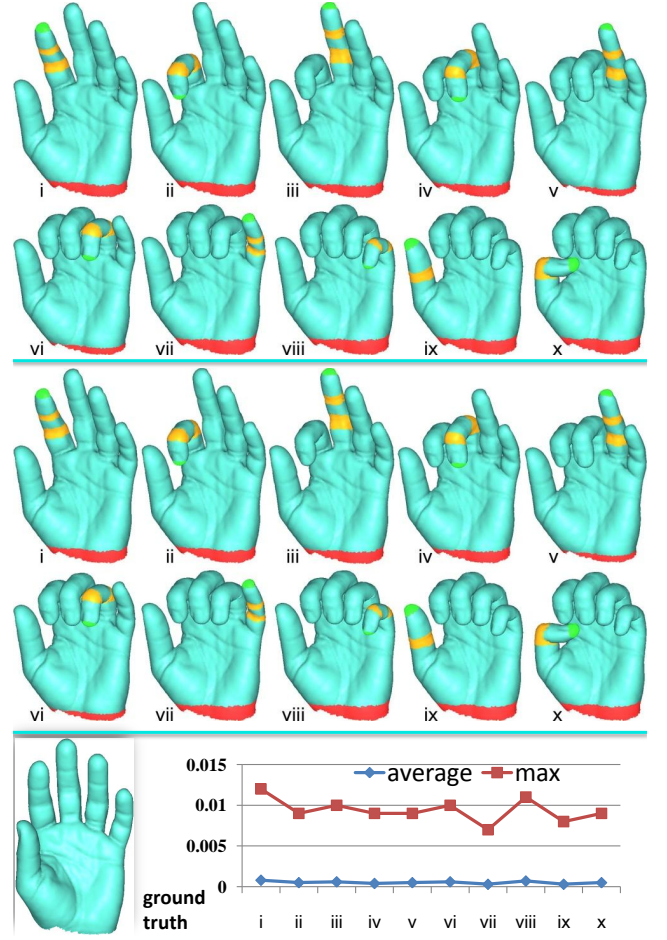


**Figure 4:** The registration of articulated hand. The partial synthetic data (up) is generated from deformation sequence, and the reconstructed shapes recover the motion (center). The reconstructed shapes are compared with relevant ground truth (bottom), the graph shows the maximum and average error distance between the ground truth and the reconstruction for each frame.

Although our method is partly taking the technique from the articulated motion capture and reconstruction method [Pekelnny and Gotsman 2008]. However, [Pekelnny and Gotsman 2008] requires the user to manually segment a range scan in advance, whereas we automatically solve for the segmentation using the transformation computed in all frames by the initial pairwise registration.

Figure 4 shows one articulated hand example. The partial synthetic data is generated from deformation sequence, and the final registered shape is produced from these partial data. We also evaluate the robustness of our reconstruction method using the ground truth, comparison shown in Figure 4 center. Quantitatively, we measured the maximum of the average distance over all frames as 0.001, the maximum of the maximum distance over all frames as 0.012 as a fraction of the bounding box diagonal.

### 5.4 3D colorful real depth scans

Complementary to the extensive evaluation presented above, we also provide a real-world example demonstrating matching using the SuperMatching. Figure 5 shows a matching result from exhibiting various transformations of KINECT camera [Kinect 2012]. The

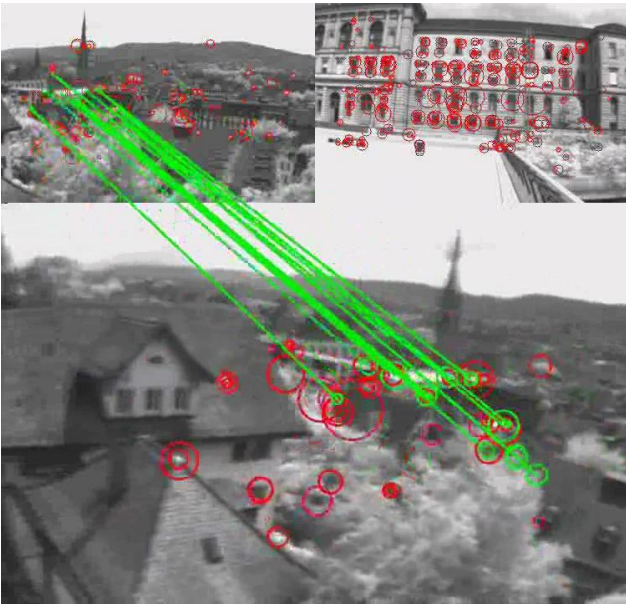


**Figure 5:** 3D colorful real depth scans from KINECT. Two given different local pre-scans are shown on the up. The real varying depth data is captured by KINECT, and one snap is listed on the bottom. The matching points are connected by the green lines.

matching with both SIFT and slippage features was performed by the SuperMatching, resulting in robust matches without significant outliers.

## 6 Conclusion

This paper has given a novel matching algorithm named SuperMatching, which tackles the classic Computer Graphics and Computer Vision problem of matching various features for cases without any assumptions. SuperMatching is an efficient higher-order matching algorithm based on the supersymmetric affinity tensor. Our main contributions are as follows. First, we use a higher-order supersymmetric affinity tensor with a compact form to express higher-order consistency constraints of features. Secondly, we derive an efficient higher-order power iteration method, which makes significant efficiency by taking advantage of supersymmetry. Finally, we also give an efficient sampling strategy for choosing feature tuples to create the affinity tensor. The experiments on both synthetic and real 2D/3D data sets show that SuperMatching is one general feature matching algorithm with accurate performance.

## References

534 AIGER, D., MITRA, N. J., AND COHEN-OR, D. 2008. 4-points  
535 congruent sets for robust pairwise surface registration. *ACM*  
536 *Transactions on Graphics* 27, 3.

537 BERG, A. C., BERG, T. L., AND MALIK, J. 2005. Shape matching  
538 and object recognition using low distortion correspondence. In  
539 *IEEE CVPR*, 26–33.

540 BOKELOH, M., BERNER, A., WAND, M., SEIDEL, H.-P., AND  
541 SCHILLING, A., 2008. Slippage features. Technical Report,  
542 WSI-2008-03, University of Tübingen,.

543 BRONSTEIN, A. M., BRONSTEIN, M. M., GUIBAS, L. J., AND  
544 OVSJANIKOV, M. 2011. Shape google: Geometric words and

545 expressions for invariant shape retrieval. *ACM Transactions on*  
546 *Graphics* 30, 1:1–1:20.

547 BROWN, B. J., AND RUSINKIEWICZ, S. 2007. Global non-rigid  
548 alignment of 3-d scans. *ACM Transactions on Graphics* 26.

549 CHANG, W., AND ZWICKER, M. 2011. Global registration of  
550 dynamic range scans for articulated model reconstruction. *ACM*  
551 *Transactions on Graphics* 30, 26:1–26:15.

552 CHERTOK, M., AND KELLER, Y. 2010. Efficient high order  
553 matching. *IEEE Transactions on Pattern Analysis and Machine*  
554 *Intelligence* 32, 2205–2215.

555 COMANICIU, D., AND MEER, P. 2002. Mean shift: A robust  
556 approach toward feature space analysis. *IEEE Transactions on*  
557 *Pattern Analysis and Machine Intelligence* 24, 603–619.

558 CONTE, D., FOGGIA, P., SANSONE, C., AND VENTO, M. 2004.  
559 Thirty years of graph matching in pattern recognition. *International*  
560 *Journal of Pattern Recognition and Artificial Intelligence*  
561 18, 3, 265–298.

562 COUR, T., SRINIVASAN, P., AND SHI, J. 2006. Balanced graph  
563 matching. In *NIPS*, 313–320.

564 DUCHENNE, O., BACH, F., KWEON, I., AND PONCE, J. 2009. A  
565 tensor-based algorithm for high-order graph matching. In *IEEE*  
566 *CVPR*, 1980–1987.

567 GELFAND, N., MITRA, N. J., GUIBAS, L. J., AND POTTSMANN,  
568 H. 2005. Robust global registration. In *Symposium on Geometry*  
569 *processing*.

570 HUTTENLOCHER, D. P., AND ULLMAN, S. 1990. Recognizing  
571 solid objects by alignment with an image. *International Journal*  
572 *of Computer Vision* 5 (November), 195–212.

573 JOHNSON, A. E., AND HEBERT, M. 1999. Using spin images for  
574 efficient object recognition in cluttered 3d scenes. *IEEE Trans-*  
575 *actions on Pattern Analysis and Machine Intelligence* 21, 5, 433–  
576 449.

577 KIM, V. G., LIPMAN, Y., AND FUNKHOUSER, T. 2011. Blended  
578 intrinsic maps. In *SIGGRAPH*, 79:1–79:12.

579 KINECT, 2012. Kinect homepage. <http://www.xbox.com/en-US/kinect>.

581 KOFIDIS, E., AND REGALIA, P. A. 2002. On the best rank-1  
582 approximation of higher-order supersymmetric tensors. *SIAM*  
583 *Journal on Matrix Analysis and Applications* 23, 3, 863–884.

584 KOLDA, T. G., AND BADER, B. W. 2009. Tensor decompositions  
585 and applications. *SIAM Review* 51, 3, 455–500.

586 LEORDEANU, M., AND HEBERT, M. 2005. A spectral technique  
587 for correspondence problems using pairwise constraints. In *International*  
588 *Conference of Computer Vision*, 1482–1489.

589 LEUTENEGGER, S., CHLI, M., AND SIEGWART, R. 2011. Brisk:  
590 Binary robust invariant scalable keypoints. In *International*  
591 *Conference of Computer Vision*.

592 LI, H., SUMNER, R. W., AND PAULY, M. 2008. Global corre-  
593 spondence optimization for non-rigid registration of depth scans.  
594 *Computer Graphics Forum (Proc. SGP)* 27, 5, 1421–1430.

595 LIPMAN, Y., AND FUNKHOUSER, T. 2009. Möbius voting for  
596 surface correspondence. *ACM Transactions on Graphics (Proc.*  
597 *SIGGRAPH)* 28, 72:1–72:12.

- 598 LOWE, D. G. 2004. Distinctive image features from scale-invariant  
599 keypoints. *International Journal of Computer Vision* 60, 2, 91–  
600 110.
- 601 OVSJANIKOV, M., MRIGOT, Q., MMOLI, F., AND GUIBAS, L.  
602 2010. One point isometric matching with the heat kernel. *Com-  
603 puter Graphics Forum (Proc. SGP)* 29, 5, 1555–1564.
- 604 PEKELNY, Y., AND GOTSMAN, C. 2008. Articulated object recon-  
605 struction and markerless motion capture from depth video. *Com-  
606 puter Graphics Forum (Proc. EuroGraphics)* 27, 2, 399–408.
- 607 PEYRÉ, G., PÉCHAUD, M., KERIVEN, R., AND COHEN, L. D.  
608 Geodesic methods in computer vision and graphics. *Foundations  
609 and Trends in Computer Graphics and Vision* 5.
- 610 SAHILLIOGLU, Y., AND YEMEZ, Y. 2011. Coarse-to-fine com-  
611 binatorial matching for dense isometric shape correspondence.  
612 *Computer Graphics Forum (Proc. SGP)* 30, 5, 1461–1470.
- 613 SUN, J., OVSJANIKOV, M., AND GUIBAS, L. 2009. A concise and  
614 provably informative multi-scale signature based on heat diffu-  
615 sion. In *Symposium on Geometry Processing*, 1383–1392.
- 616 SUN, J., CHEN, X., AND FUNKHOUSER, T. A. 2010. Fuzzy  
617 geodesics and consistent sparse correspondences for deformable  
618 shapes. *Computer Graphics Forum* 29, 5, 1535–1544.
- 619 TEVS, A., BOKELOH, M., WAND, M., SCHILLING, A., AND SEI-  
620 DEL, H.-P. 2009. Isometric registration of ambiguous and partial  
621 data. In *IEEE CVPR*, 1185–1192.
- 622 TEVS, A., BERNER, A., WAND, M., IHRKE, I., AND SEIDEL,  
623 H.-P. 2011. Intrinsic shape matching by planned landmark sam-  
624 pling. *Computer Graphics Forum* 30, 2, 543–552.
- 625 TOLER-FRANKLIN, C., BROWN, B., WEYRICH, T.,  
626 FUNKHOUSER, T., AND RUSINKIEWICZ, S. 2010. Multi-  
627 feature matching of fresco fragments. *ACM Transactions on  
628 Graphics (Proc. SIGGRAPH ASIA)* 29, 185:1–185:12.
- 629 TORRESANI, L., KOLMOGOROV, V., AND ROTHER, C. 2008.  
630 Feature Correspondence Via Graph Matching: Models and  
631 Global Optimization. In *the 10th European Conference on Com-  
632 puter Vision*, Springer-Verlag, 596–609.
- 633 VAN KAICK, O., ZHANG, H., HAMARNEH, G., AND COHEN-  
634 OR, D. 2011. A survey on shape correspondence. *Computer  
635 Graphics Forum* 30, 6.
- 636 WAND, M., ADAMS, B., OVSJANIKOV, M., BERNER, A.,  
637 BOKELOH, M., JENKE, P., GUIBAS, L., SEIDEL, H.-P., AND  
638 SCHILLING, A. 2009. Efficient reconstruction of nonrigid shape  
639 and motion from real-time 3d scanner data. *ACM Transactions  
640 on Graphics* 28, 15:1–15:15.
- 641 WANG, A., LI, S., AND ZENG, L. 2010. Multiple order graph  
642 matching. In *IEEE ACCV*, 471–482.
- 643 WINDHEUSER, T., SCHLICKWEI, U., SCHIMDT, F. R., AND  
644 CREMERS, D. 2011. Large-scale integer linear programming  
645 for orientation preserving 3d shape matching. *Computer Graph-  
646 ics Forum (Proc. SGP)* 30, 5, 1471–1480.
- 647 ZASS, R., AND SHASHUA, A. 2008. Probabilistic graph and hy-  
648 pergraph matching. In *IEEE CVPR*, 1–8.
- 649 ZENG, Y., WANG, C., WANG, Y., GU, X., SAMARAS, D., AND  
650 PARAGIOS, N. 2010. Dense non-rigid surface registration using  
651 high-order graph matching. In *IEEE CVPR*, 382–389.